Suppressing a Sea of Starlight : enabling technology for the direct imaging of exoplanets

Otten, G.P.P.L.

4 Vector Apodizing Phase Plate coronagraph: prototyping, characterization and outlook

Abstract

The Apodizing Phase Plate (APP) is a phase-only pupil-plane coronagraph that suppresses starlight in a D-shaped region from 2 to 7 λ/D around a target star. Its performance is insensitive to residual tip-tilt variations from the AO system and telescope structure. Using liquid crystal technology we develop a novel and improved version of the APP: the broadband vector Apodizing Phase Plate (vAPP). The vAPP prototype consists of an achromatic half-wave retarder pattern with a varying fast axis encoding phase structure down to 25 microns. The fast axis encodes the required phase pattern through the vector phase, while multiple twisting liquid crystal layers produce a nearly constant half-wave retardance over a broad bandwidth. Since pupil phase patterns are commonly designed to be antisymmetric, two complementary PSFs are produced with dark holes on opposite sides.

We summarize results of the characterization of our latest vAPP prototype in terms of pupil phase reconstruction and PSF contrast performance. The liquid crystal patterning technique allows us to manufacture more extreme phase patterns than was possible before. We consider phase-only patterns that yield higher contrasts and better inner working angles than previous APPs, and patterns that produce dark regions 360 degrees around the PSF core. The possibility of including a phase ramp into the coronagraph is demonstrated, which simplifies the vAPP into a single optic. This additional phase ramp removes the need for a quarter-wave plate and a Wollaston prism, and enables the simplified implementation of a vAPP in a filter wheel at a pupil-plane location. Since the phase ramp is analogous to a polarization grating, it generates a (polarized) spectrum of a planet inside the dark hole, and thus allows for instantaneous characterization of the planet.

Gilles P.P.L. Otten, Frans Snik, Matthew A. Kenworthy, Matthew N. Miskiewicz, Michael J. Escuti and Johanan L. Codona
Proc. SPIE 9151, 91511R, (2014)

4.1 Introduction

The conceptually easiest way of suppressing light of a star is by physically blocking it at the focal plane, as is done with Lyot-type focal-plane coronagraphs. Light that diffracts around this blocking element is subsequently removed by a Lyot stop in the pupil plane. More exotic designs of Lyot-type coronagraphs using amplitude and/or phase techniques have been made that show excellent contrasts, but focal-plane devices are susceptible to pointing errors and vibrations in the optical system. Therefore, additional telescope vibrations cause starlight to leak from behind the coronagraph.

A class of coronagraphs exist which are insensitive to tip-tilt variations by being located in the pupil plane. The Apodizing Phase Plate (APP) coronagraph is a pupil plane coronagraph that only uses phase to suppress the diffraction pattern on one side of the star (Codona et al., 2006; Kenworthy et al., 2007). The power of the APP was most dramatically demonstrated in the case of VLT/NACO before 2011 when the star drifted in a circle during observations when pupil tracking was enabled, reducing the efficiency of Lyot-type coronagraphs until a fix was implemented (Girard et al., 2012). The APP coronagraph was not susceptible to this drifting. Residual tip-tilt variations remain an important limiting factor in coronagraphs installed in the latest generation of planet-finding instruments (e.g., GPI (Macintosh et al., 2014), SPHERE, SCExAO (Singh et al., 2014)). Substantial investments have to be made in order to create a system that keeps these variations at an acceptable level.

Despite the successes of the APP coronagraph (Kenworthy et al., 2007; Quanz et al., 2010; Quanz et al., 2013) and its ease of implementation, it has some limitations that are partly due to the manufacturing method. The commonly stated limitations of the APP coronagraph are the suppression of only one side of the PSF, the dependence of the phase delay on the wavelength, and limited contrast. We can overcome all these problems in by using a different manufacturing technique based on patterned liquid crystal retarders. The so-called vector APP (Snik et al., 2012; Otten et al., 2014) produces two complementary PSFs with broadband suppression $\frac{\delta\lambda}{\lambda} \approx 100\%$. Moreover this manufacturing technique allows for phase patterns that deliver higher raw contrast.

4.2 Vector Apodizing Phase Plate prototype

The classical Apodizing Phase Plate uses optical path difference to induce a phase as a function of pupil position. The phase delay arises from a varying optical path difference. This phase is highly dependent on the wavelength and any deviation from the design wavelength will create a phase pattern that is not optimal for suppression of starlight.

Instead of using optical path differences to create a phase delay across the pupil, the vAPP works with the vector phase, also known as Pancharatnam-Berry phase (Pancharatnam, 1956; Berry, 1984; Mawet et al., 2009), which arises when a beam of light hits a half-wave plate (HWP). This beam is decomposed into the two different circular polarization states. The HWP flips the handedness and imposes a phase delay depending on the orientation of the fast axis of the HWP. The vector phase $\Delta\phi$ of a birefringent retarder is given by

$$\Delta\phi = \pm 2 \cdot \theta \tag{4.1}$$

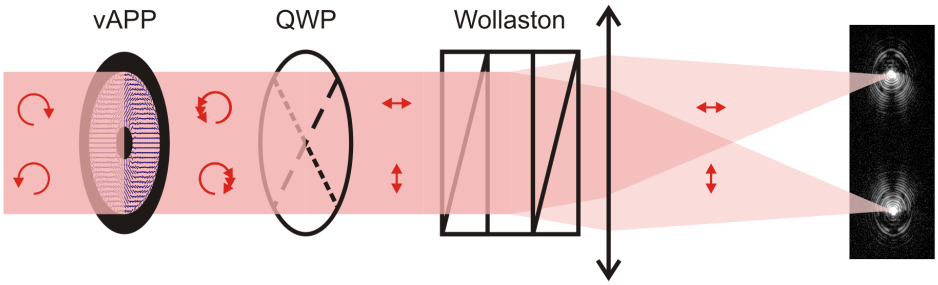

Figure 4.1: Working principle of the vAPP. Circular polarized light passing through the vAPP flips handedness and picks up a phase. The combination of quarter-wave plate and Wollaston prism splits the light based on circular polarization forming two PSFs on the focal plane. The focal plane image on the right was taken with the lab setup.

where θ is the local fast axis and the sign depends on the handedness of circular polarization. A beam-splitting step is required to separate the two circular polarization states with opposite phase patterns. This is implemented in Figure 4.1 with a quarter-wave plate and a Wollaston prism.

The phase delay of Equation 4.1 does not depend on the wavelength of the light and therefore is achromatic. When the HWP is not completely half-wave, a fraction of light will leak through unaberrated and contaminates the suppressed beam with the original PSF. Therefore, in order to be truly achromatic this HWP needs to be half-wave across the required wavelength range. Using liquid crystal technology it is possible to create patterned vector phase elements which retardance can be made achromatic over a large wavelength range. The patterning is enabled by a direct-write technique (Miskiewicz and Escuti, 2014) and the achromatization is accomplished with Multi-Twist Retarders (MTRs) (Komanduri et al., 2013). The vAPP consists of a substrate and a photoalignment polymer that aligns itself to the linear polarization direction of a UV laser that writes the desired pattern. Additional layers of chromatic birefringent liquid crystal align themselves with the layer underneath. By combining several layers together in a predetermined way, an increasingly achromatic retarder is built (Komanduri et al., 2013).

A prototype vector APP was constructed using these two manufacturing methods. It was specified to be within 11 degrees from half-wave retardance over the wavelength range of 500 to 900 nm. The active surface with the APP phase pattern has a 5.5 mm diameter with a 20% secondary obscuration. An opaque mask of the same dimensions was made, aligned to the HWP under a microscope and bonded with optical glue (Otten et al., 2014).

The properties of the prototype were verified using a polarimetric imaging method (Otten et al., 2014) and uses 8 images of the optic in between two polarizers at varying position angles. To assess the coronagraphic performance, the prototype was placed in an optical setup following the layout of Figure 4.1. The point spread function (PSF) was measured by looking at a white fiber-fed light source using narrowband filters from 500 to 800 nm. The corresponding PSFs for different wavelengths can be seen in Figure 4.2. To demonstrate the raw contrast that can be reached with this plate, the PSFs at 750 nm were converted to contrast curves by azimuthally averaging the flux in the dark hole and dividing it by the peak flux of the PSF. Both measured PSFs match each other well. The model of the contrast curve includes the non-ideal properties of

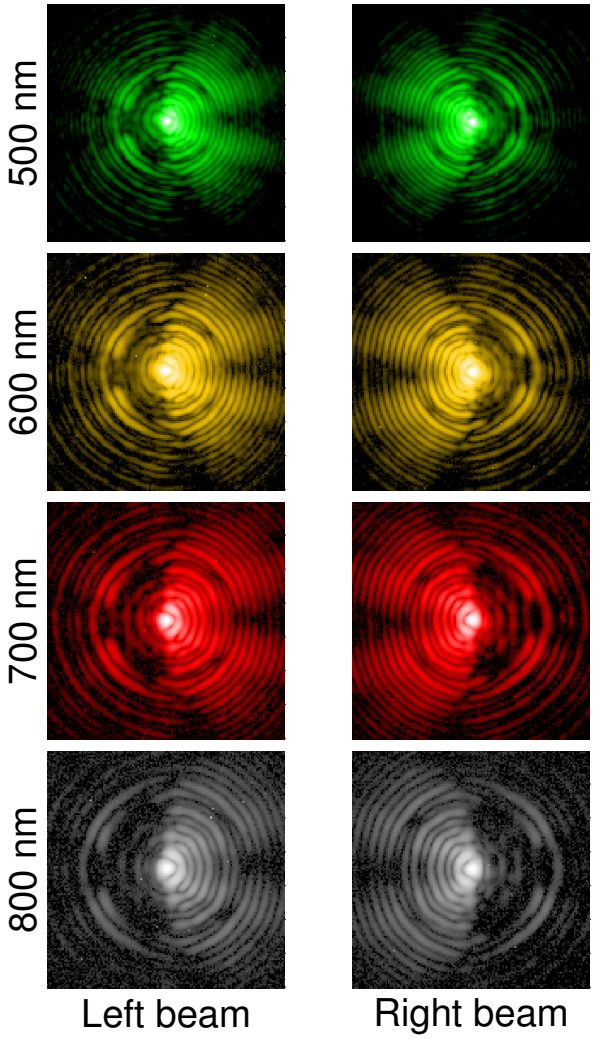

Figure 4.2: Simultaneously taken images of Left and Right PSFs from 500 to 800 nanometers showing a dark hole at all wavelengths on both sides of the star.

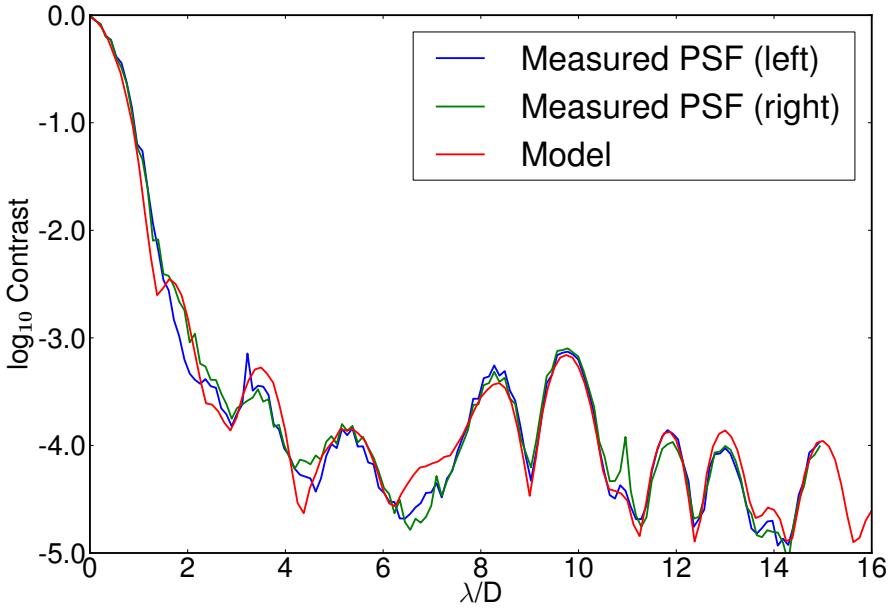

Figure 4.3: Contrast of Left and Right PSFs measured in a wedge centered on the dark hole compared to a forward model that is based on the measured properties of the coronagraph.

the vAPP as measured in the lab. This model matches the measured PSF data (as seen in Fig. 4.3) and confirms the validity of our model.

The one factor that limits the contrast most is the retardance offset from half-wave as presented in Figure 4.4. The same figure also presents designs with more layers that yield superior retardance performance. Future revisions should therefore focus on improving the retardance or mitigating the effect it has on the contrast.

4.3 New opportunities

The liquid crystal patterning technique gives high control over the phase of the optic, especially in terms of spatial frequencies that were not offered by the traditional diamond turning technique. It also allows for a natural match with polarization tricks and polarimetric techniques (Snik et al., 2014). This gives a lot of options to improve the coronagraph.

4.3.1 Integration of beam splitting

The vector Apodizing Phase Plate requires a combination of a quarter-wave plate and a Wollaston prism in order to split based on the circular polarization (Figure 4.1). This adds two extra optical elements in the path that have to be both broad-band and properly aligned. Therefore, despite

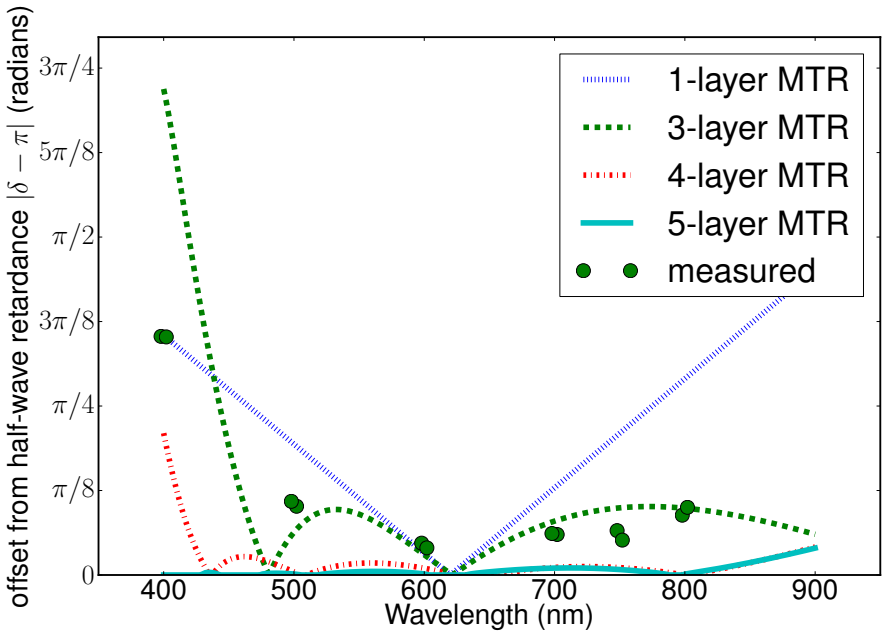

Figure 4.4: Offset from half-wave retardance of the plate as theoretically expected for several layered designs and measured in the lab. The three-layer recipe denoted with the green line was used for the optic that was tested. The corresponding measurements are shown in green circles.

being an improved version of the APP it complicates the installation at telescopes.

Another way of splitting the PSFs is by applying a tip-tilt phase ramp to the APP phase pattern itself, as is shown in Figure 4.5. Depending on the circular polarization of the beam it will either deflect in one direction or the other while still maintaining the APP phase pattern. Since the splitting is now done by the tip-tilt phase, the QWP and Wollaston are no longer needed. The errors associated with them are consequently absent. The coronagraph is again reduced to a single optic in the pupil plane.

Any leakage term is not deflected and passes straight through, forming an image between the two APP PSFs, and avoiding contrast loss in the APP PSFs. It is possible to observe outside of the designed wavelength range in exchange for greater leakage losses. The phase ramp is a polarization grating (Packham et al., 2010; Oh and Escuti, 2008) and therefore disperses the split PSFs as a function of wavelength. This limits the spectral bandwidth that can be used for observing due to wavelength smearing, although a single optic can still be used with multiple narrow/intermediate band filters.

In Figure 4.6 we simulate the effect of a 10% bandwidth beam of light through this optic with a retardance of 0.45 waves. The leakage term of the half-wave plate ends up between the two APP PSFs and does not impact the contrast. It is also possible to exploit this splitting effect to obtain low resolution spectra of the planet.

For the three layer device, the leakage term contains a few percent of the total light through the

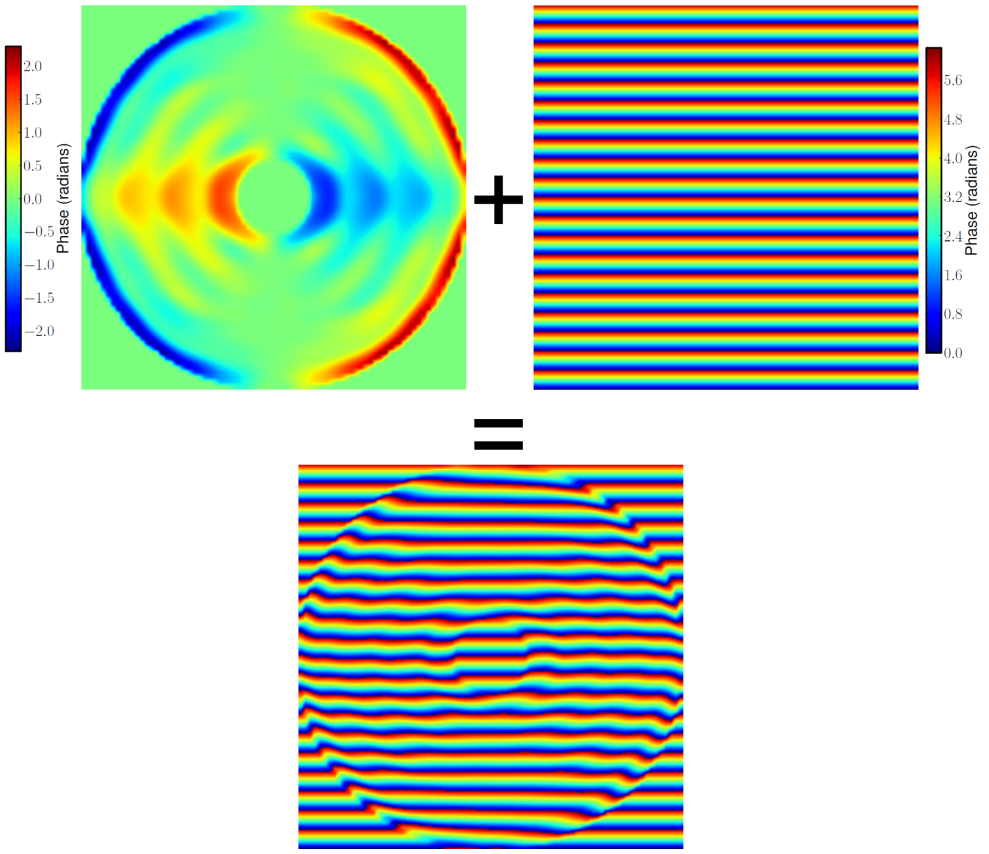

Figure 4.5: The two top images show a phase pattern for creating a dark hole on one side of the star and a tip-tilt phase pattern that moves the star to one side. The combined phase pattern in the bottom panel therefore suppresses the starlight in complementary sides of the PSF and simultaneously splits the beams.

coronagraph. This third unaberrated PSF can be used as a photometric and astrometric reference source, as it is not saturated and remains unaltered by the phase pattern on the plate. Furthermore, it opens up the possibility of using phase diversity wavefront estimation methods to measure the wavefront in the focal plane. (Gonsalves, 1982; Blanc et al., 2003; Riaud, P. et al., 2012)

4.3.2 Aggressive phase patterns

The direct-write method offers control over the phase with a spatial resolution of at least 10 microns (Miskiewicz and Escuti, 2014). In contrast to diamond-turning methods, the phase pattern can be made with rapidly changing phases over very small spatial scales. It is therefore possible to realize phase patterns that have higher contrast than the diamond-turning optimized patterns of the previous APP. Many phase pattern solutions with theoretically high contrasts have been obtained (Carlotti, 2013; Codona and Angel, 2004). All of these are anti-symmetric and therefore produce two PSFs with complementary dark holes in a vector APP configuration.

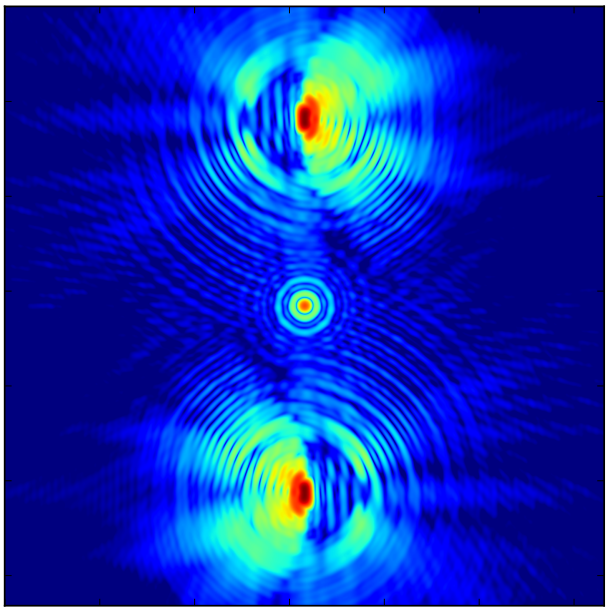

Figure 4.6: Simulated PSF of the APP pattern with a ramp of phase added. The bandwidth was set to 10% and the retardance of the HWP was set to 0.45 waves. The leakage term ends up between the two PSFs and consequently does not impact the contrast.

4.3.3 360 degree suppression

In the process of looking for APP solutions, phase-only solutions that are not anti-symmetric were found (Codona, private communications). One specific phase design that was encountered produces a 360 degree dark ring around the PSF core. A vAPP prototype with this 360 degree pattern was made using the aforementioned manufacturing method and is shown in Figure 4.7.

The theoretical PSF for this phase pattern is shown in Figure 4.8. Note that for a vAPP implementation this PSF is only obtained for one circular polarization. The Strehl ratio of this design is 0.176 and has a contrast of $\approx 10^{-5}$ in a 360 degree region between 2 and 8 λ/D. To verify the reality of this solution we implemented this phase pattern with a spatial light modulator (Korkiakoski et al., 2013) with the preliminary result for the PSF shown in Figure 4.9. Further research with the 360 degree vAPP is ongoing.

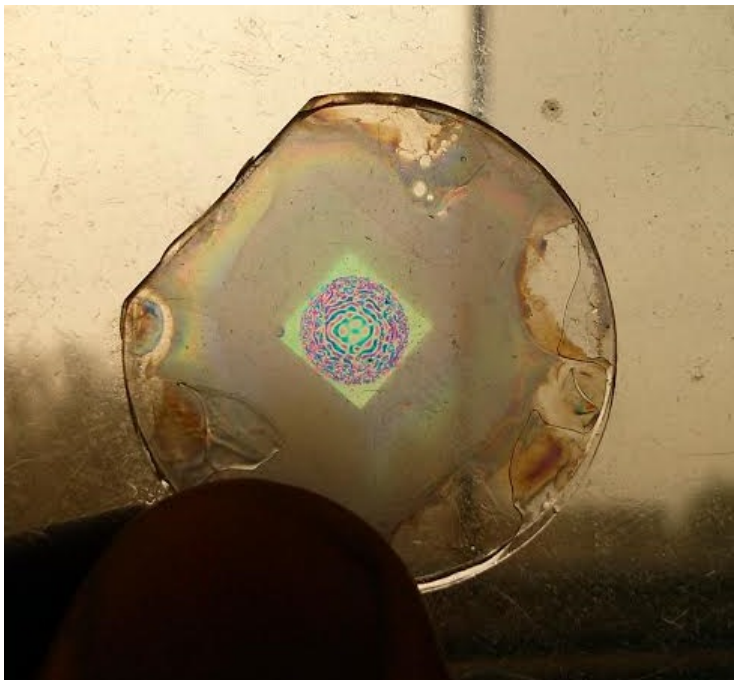

Figure 4.7: Image of 360 degree suppressing phase pattern made using the liquid crystal patterning technique. It can be seen that the pattern at the edge of the phase pattern is very aggressive and could not have been manufactured without the direct-write method.

4.4 Conclusion

In this paper we describe the prototyping of the first achromatic vector APP and its characterization. We demonstrate that the coronagraph meets its design specifications between 500 and 800 nanometers and provides $10^{-3.8}$ contrast in complementary dark holes between 2 and 7 λ/D. After successful prototyping we further develop the vAPP concept. By adding a phase ramp to the APP pattern, it is possible to make a simplified version of the vAPP that can be easily implemented into existing telescopes at the cost of limited spectral bandwidth. This version is extremely robust against offsets from half-wave retardance. The manufacturing technique allows us to locally encode a certain phase with a very high spatial resolution which allows us to create phase patterns that have a better contrast than the previous versions and it is now possible to create phase patterns with 360 degree suppression around the PSF core.

The use of the MTR class of half-wave plates is not limited to the visible band but by choosing a different substrate and liquid crystal compounds devices can also be made to work at the NIR/Thermal IR. We are currently implementing vector APP coronagraphs at large telescopes such as the LBT and Magellan to directly image extrasolar planets at infrared wavelengths.

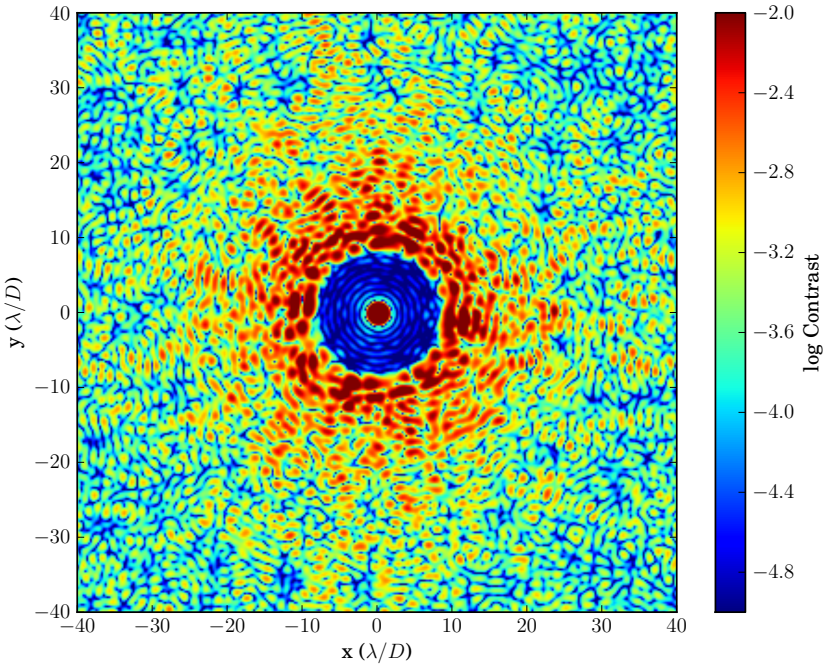

Figure 4.8: Theoretical PSF of a 360 degree suppressing APP pattern. Between 2 and 7 λ/D the contrast is about 10^{-5}.

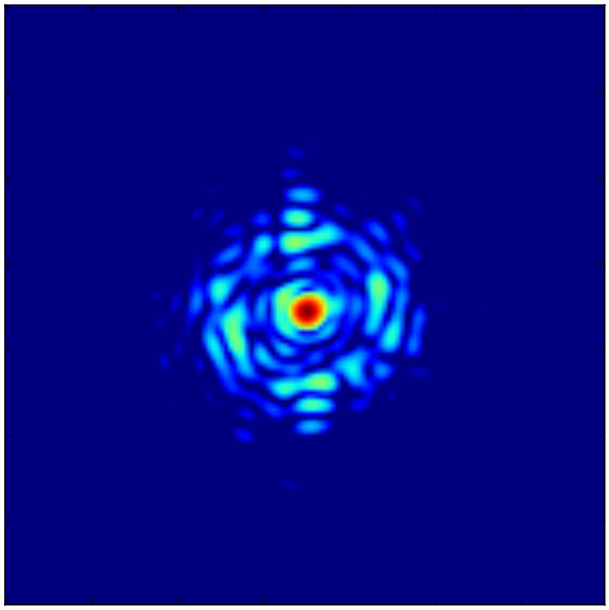

Figure 4.9: Measured laboratory PSF of a 360 degree suppressing APP pattern simulated with a spatial light modulator. It is seen that the light is suppressed in a circular region and moved outward.

Acknowledgments

The authors would like to thank Alex Pietrow and Visa Korkiakoski for their support with the laboratory setup. This work is part of the research programme Instrumentation for the E-ELT, which is partly financed by the Netherlands Organisation for Scientific Research (NWO).

References

Berry, M. V. (1984). Quantal Phase Factors Accompanying Adiabatic Changes. *Royal Society of London Proceedings Series A*, 392:45–57.

Blanc, A., Fusco, T., Hartung, M., Mugnier, L., and Rousset, G. (2003). Calibration of naos and conica static aberrations. *Astronomy and Astrophysics*, 399(1):373–383.

Carlotti, A. (2013). Apodized phase mask coronagraphs for arbitrary apertures. *A&A*, 551:A10.

Codona, J. L. and Angel, R. (2004). Imaging Extrasolar Planets by Stellar Halo Suppression in Separately Corrected Color Bands. *ApJ*, 604:L117–L120.

Codona, J. L., Kenworthy, M. A., Hinz, P. M., Angel, J. R. P., and Woolf, N. J. (2006). A high-contrast coronagraph for the MMT using phase apodization: design and observations at 5 microns and 2 λ/D radius. In *Society of Photo-Optical Instrumentation Engineers (SPIE) Conference Series*, volume 6269 of *Society of Photo-Optical Instrumentation Engineers (SPIE) Conference Series*.

Girard, J. H. V., O'Neal, J., Mawet, D., Kasper, M., Zins, G., Neichel, B., Kolb, J., Christiaens, V., and Tourneboeuf, M. (2012). Image quality and high contrast improvements on vlt/naco. In *Proc. SPIE*, volume 8447, pages 84470L–84470L–14.

Gonsalves, R. A. (1982). Phase retrieval and diversity in adaptive optics. *Optical Engineering*, 21(5):215829–215829–.

Kenworthy, M. A., Codona, J. L., Hinz, P. M., Angel, J. R. P., Heinze, A., and Sivanandam, S. (2007). First On-Sky High-Contrast Imaging with an Apodizing Phase Plate. *ApJ*, 660:762–769.

Komanduri, R. K., Lawler, K. F., and Escuti, M. J. (2013). Multi-twist retarders: broadband retardation control using self-aligning reactive liquid crystal layers. *Opt. Express*, 21(1):404–420.

Korkiakoski, V., Doelman, N., Codona, J., Kenworthy, M., Otten, G., and Keller, C. U. (2013). Calibrating a high-resolution wavefront corrector with a static focal-plane camera. *Appl. Opt.*, 52:7554.

Macintosh, B., Graham, J. R., Ingraham, P., Konopacky, Q., Marois, C., Perrin, M., Poyneer, L., Bauman, B., Barman, T., Burrows, A. S., Cardwell, A., Chilcote, J., De Rosa, R. J., Dillon, D., Doyon, R., Dunn, J., Erikson, D., Fitzgerald, M. P., Gavel, D., Goodsell, S., Hartung, M., Hibon, P., Kalas, P., Larkin, J., Maire, J., Marchis, F., Marley, M. S., McBride, J., Millar-Blanchaer, M., Morzinski, K., Norton, A., Oppenheimer, B. R., Palmer, D., Patience,

J., Pueyo, L., Rantakyro, F., Sadakuni, N., Saddlemyer, L., Savransky, D., Serio, A., Soummer, R., Sivaramakrishnan, A., Song, I., Thomas, S., Wallace, J. K., Wiktorowicz, S., and Wolff, S. (2014). First light of the gemini planet imager. *Proceedings of the National Academy of Sciences*, 111(35):12661–12666.

Mawet, D., Serabyn, E., Liewer, K., Hanot, C., McEldowney, S., Shemo, D., and O'Brien, N. (2009). Optical Vectorial Vortex Coronagraphs using Liquid Crystal Polymers: theory, manufacturing and laboratory demonstration. *Optics Express*, 17:1902–1918.

Miskiewicz, M. N. and Escuti, M. J. (2014). Direct-writing of complex liquid crystal patterns. *Opt. Express*, 22(10):12691–12706.

Oh, C. and Escuti, M. J. (2008). Achromatic diffraction from polarization gratings with high efficiency. *Opt. Lett.*, 33(20):2287–2289.

Otten, G. P. P. L., Snik, F., Kenworthy, M. A., Miskiewicz, M. N., and Escuti, M. J. (2014). Performance characterization of a broadband vector apodizing phase plate coronagraph. *Opt. Express*, 22(24):30287–30314.

Packham, C., Escuti, M., Ginn, J., Oh, C., Quijano, I., and Boreman, G. (2010). Polarization gratings: A novel polarimetric component for astronomical instruments. *Publications of the Astronomical Society of the Pacific*, 122(898):pp. 1471–1482.

Pancharatnam, S. (1956). Generalized theory of interference, and its applications. part i. coherent pencils. In *Proceedings of the Indian Academy of Sciences, Section A*, volume 44,5, pages 247–262. Indian Academy of Sciences.

Quanz, S. P., Amara, A., Meyer, M. R., Kenworthy, M. A., Kasper, M., and Girard, J. H. (2013). A Young Protoplanet Candidate Embedded in the Circumstellar Disk of HD 100546. *ApJ*, 766:L1.

Quanz, S. P., Meyer, M. R., Kenworthy, M. A., Girard, J. H. V., Kasper, M., Lagrange, A.-M., Apai, D., Boccaletti, A., Bonnefoy, M., Chauvin, G., Hinz, P. M., and Lenzen, R. (2010). First results from very large telescope naco apodizing phase plate: 4 um images of the exoplanet beta pictoris b. *The Astrophysical Journal Letters*, 722(1):L49.

Riaud, P., Mawet, D., and Magette, A. (2012). Instantaneous phase retrieval with the vector vortex coronagraph. *A&A*, 545:A151.

Singh, G., Guyon, O., Baudoz, P., Jovanovich, N., Martinache, F., Kudo, T., Serabyn, E., and Kuhn, J. G. (2014). Lyot-based low order wavefront sensor: implementation on the subaru coronagraphic extreme adaptive optics system and its laboratory performance. In *Proc. SPIE*, volume 9148, pages 914848–914848–9.

Snik, F., Otten, G., Kenworthy, M., Mawet, D., and Escuti, M. (2014). Combining vector-phase coronagraphy with dual-beam polarimetry. In *Proc. SPIE*, volume 9147, pages 91477U–91477U–12.

Snik, F., Otten, G., Kenworthy, M., Miskiewicz, M., Escuti, M., Packham, C., and Codona, J. (2012). The vector-APP: a broadband apodizing phase plate that yields complementary PSFs. In *Proc. SPIE*, volume 8450.